Surface analytical facility at NPL, New Delhi

B. R. Chakraborty*, Pardeep Mohan, S. M. Shivaprasad, D. R. Sharma, C. Anandan, A. C. Gupta and A. K. Raychaudhuri

National Physical Laboratory, Dr K. S. Krishnan Road, New Delhi 110 012, India

The Surface Physics group at the National Physical Laboratory (NPL), New Delhi, has established different surface characterization facilities, viz. Low Energy Electron Diffraction (LEED), Electron Energy Loss Spectroscopy (EELS), Auger Electron Spectroscopy (AES), X-ray Photoelectron Spectroscopy (XPS) and Secondary Ion Mass Spectrometry (SIMS). The group has been involved in studying the surface and interface of metals and semiconductors to understand the bond formation, surface crystal structure, chemical states, impurity profiles and interfacial diffusion, etc. using the above techniques. In addition, this group is also involved in establishment of vacuum standards down to a pressure of 10^{-6} Pa. A few such recent case studies have been described briefly in this article.

Introduction

Surface science and UHV-related activities at the National Physical Laboratory (NPL) are focused around three principal tasks:

i) Establishment of primary vacuum standards which currently work down to 10^{-6} Pa.
ii) Analytical characterization of surfaces and interfaces using spectroscopic techniques like Auger Electron Spectroscopy (AES), X-ray Photoelectron Spectroscopy (XPS) and depth resolved technique like Secondary Ion Mass Spectrometry (SIMS).
iii) Study of monolayer growth of metals on reconstructed semiconductor surfaces using Low Energy Electron Diffraction (LEED), Electron Energy Loss Spectroscopy (EELS), AES and XPS.

In the following we will provide a brief glimpse of our work in these areas.

Experimental facilities

The following vacuum and surface science experimental facilities are available at NPL.

*For correspondence.

The orifice flow system of primary vacuum standard

NPL being a national metrology institute has the responsibility to maintain primary standards of pressure down to 10^{-6} Pa. At present it generates the primary scale from 10^{5} Pa to 10^{-6} Pa using the Ultrasonic Interferometer Manometer (UIM), the Static Expansion Apparatus (SEA) and the Orifice Flow System (OFS), the last one being of interest in the area of high vacuum. In addition, NPL also provides calibrations in the complete range traceable to the primary standards.

In the OFS[1,2], a test gas at a flow rate Q is pumped out of an orifice of known conductance C connected across two chambers, generating a pressure p in the calibration chamber

$$p = \frac{Q}{C} + p' = \frac{Q}{C}\left(1 + \frac{C}{S_p}\right), \tag{1}$$

p' and S_p being the pressure and pumping speed, respectively in the chamber below the orifice. Thus p can be calculated provided Q, C and p' or S_p are known. Figure 1 is a photograph of the OFS. Both the chambers are spherical in shape to ensure a Maxwellian velocity distribution and can be evacuated to ultimate pressures of 10^{-8} Pa.

The value of the orifice conductance is obtained from the equation.

$$\frac{1}{C} = \sqrt{\frac{2\pi M}{RT}} \cdot \frac{1}{a}\left[\frac{(1-a)/A}{K} + \left(1 + \frac{3}{4}\cdot\frac{1}{D}\right)\frac{a}{A}\right], \tag{2}$$

where a is the area of the orifice, A, l and D are the area, length, and diameter, respectively of the tube in which the disk containing the orifice is mounted and K is a dimensionless factor dependent on the ratio a/A. The effective conductance of the orifice assembly has also been determined experimentally and agrees within 0.1% of the theoretical value[1].

A constant volume flow meter[3] determines the flow rate from the rate of rise of pressure dP/dt measured in a volume V as

$$Q = V\,(dP/dt)\ \text{Pa}.l.s^{-1}.$$

Figure 1. Photograph of the NPL orifice flow system.

Calibration pressures as low as 2×10^{-5} Pa can be generated in the upper chamber of the orifice flow system by admitting gas at flow rates $\geq 10^{-6}$ Pa.*l*.s^{-1} and making use of the eq. (1). The measurement uncertainty associated with flow rates lower than about 10^{-6} Pa.*l*.s^{-1} increases beyond 1% due to outgassing from the flowmeter. Therefore, for generating pressures below 2×10^{-5} Pa, the flow division technique is employed. The expanded uncertainty in the pressure generated while the flowmeter is valved into the upper chamber is 2.25% while that using the flow division technique is estimated to be 4.5%.

Secondary electron spectroscopies

The LEED, EELS and AES techniques are installed in an UHV system (Varian, VT112) capable of an operating pressure of 5×10^{-11} torr. The LEED is obtained through a 4-grid optics fitted with co-axial 3-keV electron gun and a direct view hemispherical phosphor screen. The EELS and AES are obtained from a cylindrical mirror analyser (CMA) with an energy resolution of 0.2% and a 10 keV electron gun. A 0–3 keV Ar^+ ion gun is used for sputter cleaning and erosion into depth layer by layer.

The XPS is a PHI 1257 Perkin Elmer model equipment fitted with a dual anode X-ray source for primary beam (Al K_α and Mg K_α), a 0–5 keV Ar^+ ion source for sputter cleaning and a hemispherical capacitor type energy analyser with single channel detector capable of an energy resolution up to 25 meV. An electron gun (0–4 keV) is also available in the main analysis chamber to perform AES. The operating pressure in the main chamber available is ~ 10^{-10} torr. The samples are introduced through a fast entry load lock system.

Secondary ion mass spectrometry

The SIMS is an ultra-high vacuum quadrupole ion microprobe, model MIQ256, CAMECA-RIBER. It is equipped with three different ion sources, viz. liquid metal ion (Ga^+), duo-plasmatron (O_2^+) and micro-focus Cs^+ ion source and the spectrometer has a mass range of 1–300 amu. The analysis chamber base pressure is ~10^{-11} torr while the preparation chamber (~ 10^{-8} torr) connected to the analysis chamber allows fast sample entry as well as the possibility of preparing tailor-made samples. The data acquisition and processing is done through a computer interface (HP workstation). The different modes in which the MIQ 256 can work are: (i) survey spectra or bar graph, (ii) depth profile, (iii) chemical imaging, 2D and 3D and (iv) static SIMS (Ga^+, 60 pA).

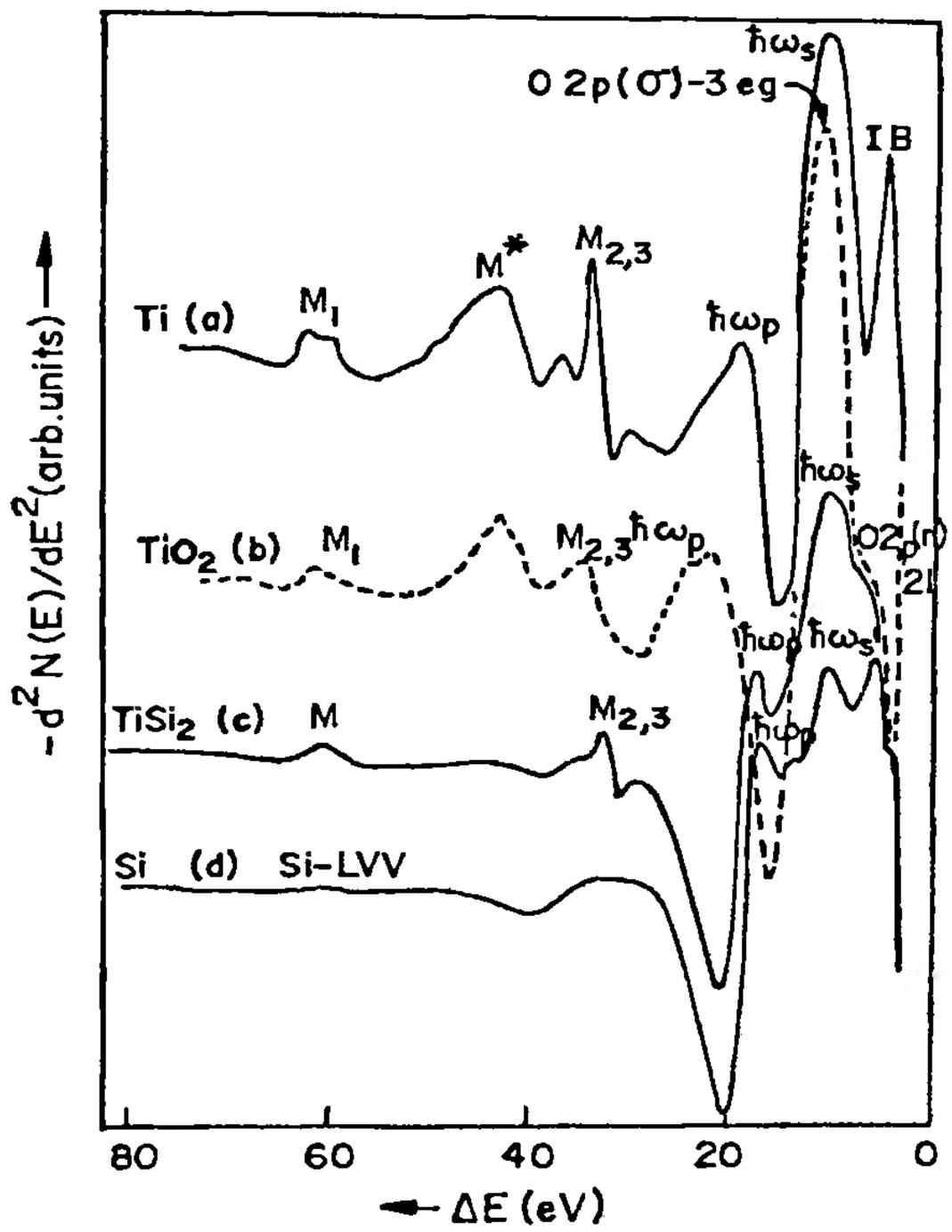

Figure 2. EELS spectra of *a*, clean Ti; *b*, TiO_2; *c*, $TiSi_2$; *d*, Si in the 0–80 eV region. The primary beam energy is 150 eV, incident at 60° to the sample normal. M* is the quasiatomic 3p-3d transition.

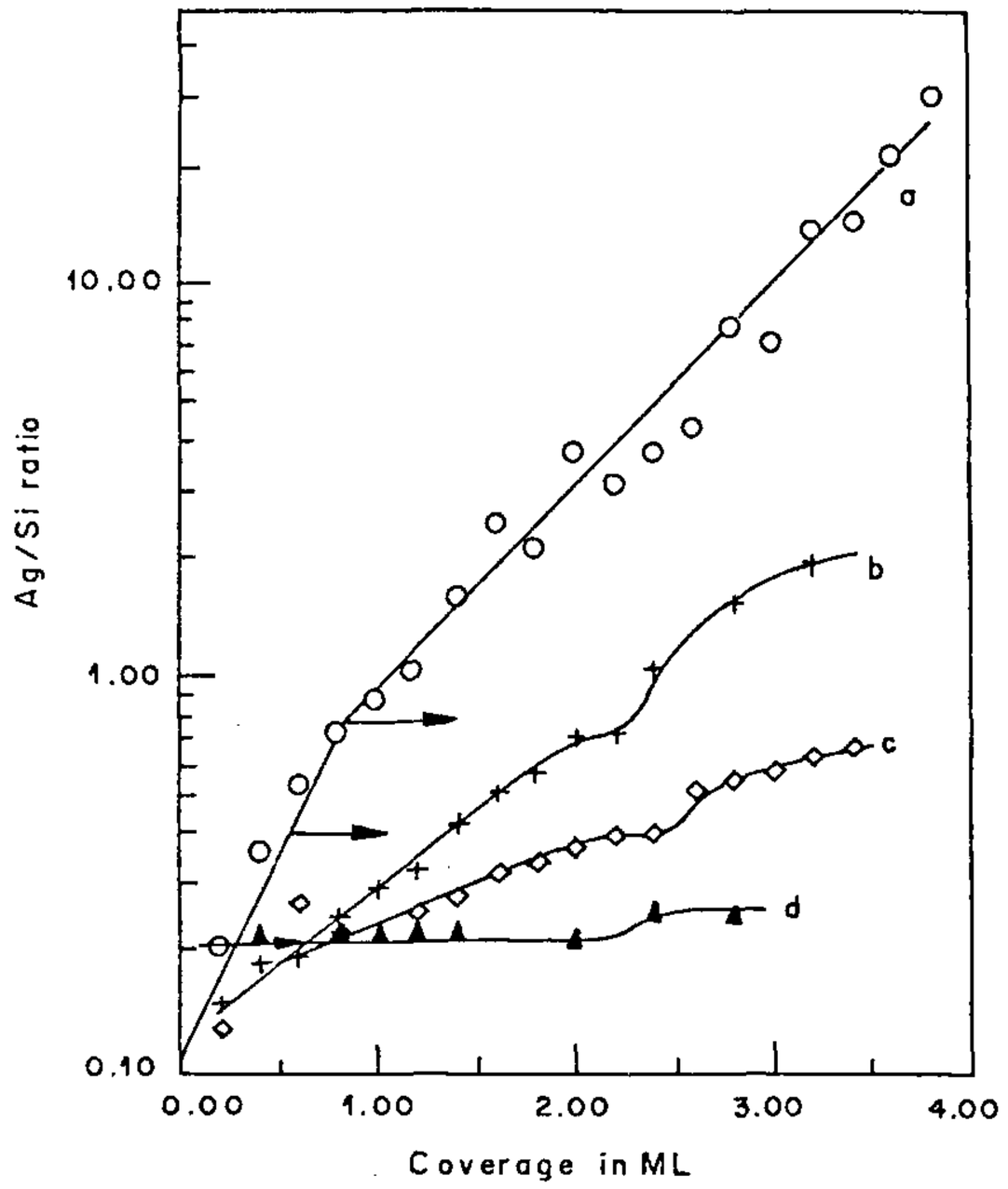

Figure 3. Ag uptake curve shown by plotting the Ag(LMM)/Si(LVV) peak intensity ratio, obtained for different substrate temperatures: *a*, O, room temperature; *b*, +, 100°C; *c*, ✧, 150°C; and *d*, ▲, 250°C.

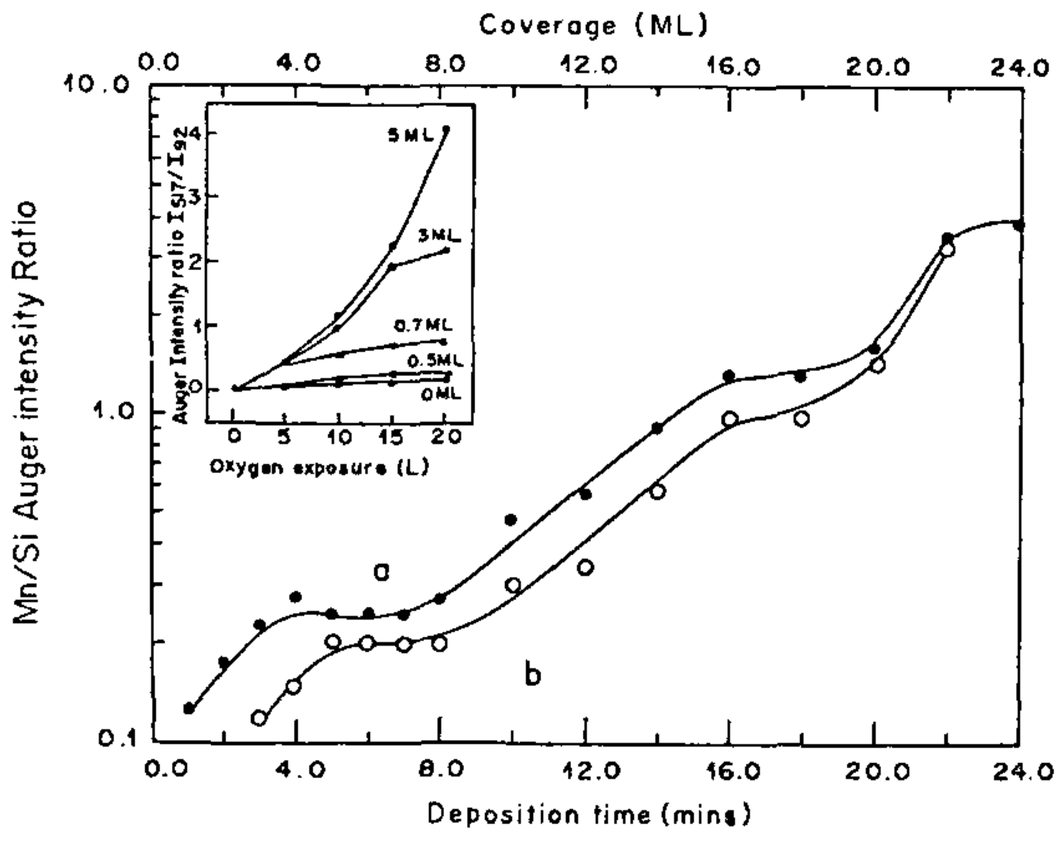

Figure 4. AES peak ratio *a*, $I_{Mn}(40)/I_{Si}(91)$ and *b*, $I_{Mn}(589)/I_{Si}(91)$ as a function of deposition time at RT (deposition rate = 1.0 monolayer min^{-1}). (Inset) Plot of O(KLL)/Si(LVV) peak intensity ratio for different coverages of Mn on Si vs oxygen exposure measured in Langmuir.

Representative results

Secondary electron spectroscopies (EELS, AES, XPS, LEED)

Study of oxidation and silicidation of some transition metals (Ti, Ta, Mo, and Cu) by electron impact autoionization process: Transition metal silicides and oxides are widely used in semiconductor device fabrication. Work was undertaken to understand the bonding process in these materials. In the EELS spectra of Ti and $TiSi_2$ it was observed that a special feature at 45 eV exists for Ti while it almost vanishes in $TiSi_2$ (Figure 2). This observation was further probed taking TiO_2 also into consideration for the bonding nature of Ti, which has two d-electrons in the valence band. The features due to the autoionization process [3p → 3d] in Ti can be observed both in EELS and AES spectra, which exist in Ti and TiO_2, but vanish in $TiSi_2$. This result has been explained in terms of empty Density of States (DOS) available in the Ti d-band, which exist or increase in Ti or TiO_2 to increase the autoionization probability, while decrease due to d-p hybridization of Si p and Ti d electrons because of covalent nature of bonding in $TiSi_2$. This model was further extended to other transition metals like Ta, Mo and Cu with different d-band occupancy[4,5].

Study of monolayer growth of silver and manganese on reconstructed surface of silicon: We have performed epitaxial thin metal film growth experiments on semiconductor surfaces to probe the formation, composition, electronic and geometric structures of the interfacial region. We have used a Knudsen cell for molecular beam growth and characterized the growth *in situ* with AES, LEED, ELS and X-ray Photo-electron Diffraction (XPD).

The Ag/Si system[6,7]: Though considered as a prototype (model) non-interacting system, the coverage and structure of the $(\sqrt{3} \times \sqrt{3})$Ag/Si interface has remained controversial. The RT growth proceeds in pseudomorphic Frank–van der Merwe mode, but at higher substrate temperatures the $(\sqrt{3} \times \sqrt{3})$-R30 structure is formed for Ag coverages of 0.33, 0.66 and 1.0 ML (Figure 3). We propose an answer to the controversy that depending on the substrate temperature, three different atomic arrangements can result in the same LEED symmetry.

The Mn/Si system[8,9]: At RT the first system grows in the Volmer–Weber mode at higher deposition rates and in the Frank–van der Merwe (1 × 1) mode for several layers at lower rates. At high coverages, the $(\sqrt{3} \times \sqrt{3})$ silicide phase is observed. However, we have also formed high quality Mn-silicide by the template method at temperatures much less than those for the bulk (Figure 4). At RT, the presence of minute amounts of Mn is observed to dramatically increase the oxygen uptake, which readily forms silicon dioxide. We propose that the Mn sites break the O–O bonds and promote reaction with underlying Si atoms.

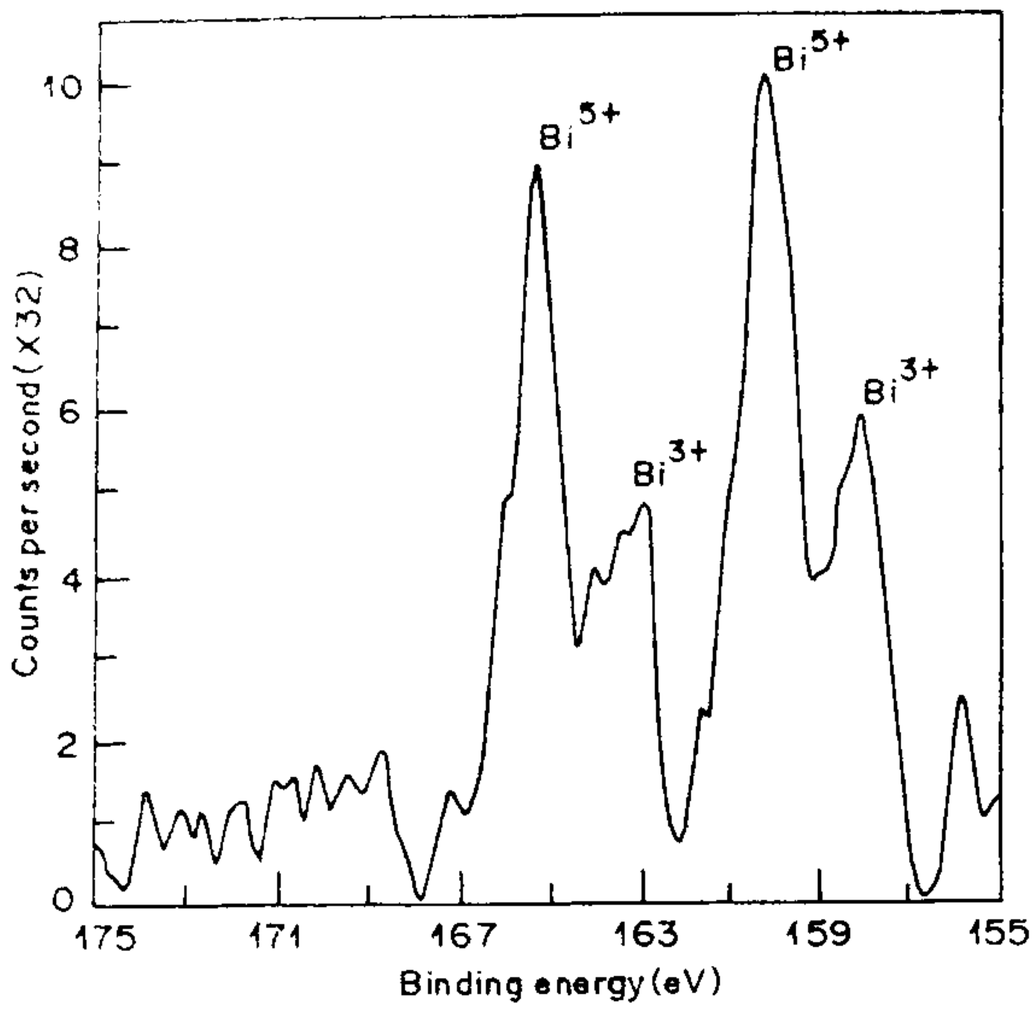

Figure 5. XPS spectrum of barium hexaferrite of composition $BaO5.6Fe_2O_30.4Bi_2O_3$ after sputtering of the sample surface showing Bi-$4f_{5/2}$ and Bi-$4f_{7/2}$ lines with splits for Bi^{5+} and Bi^{3+} contributions.

Mixed valency character of bismuth in ferrite lattices: The bismuth substituted hexaferrites [$Ba0.(6-x)Fe_2O_3.xBi_2O_3$ with $0 \le x \le 0.4$] exhibit more than two orders of magnitude higher dc electrical conductivity than that of the pure one. This is believed to arise due to an increase in the concentration of Fe^{2+} ions as a result of the presence of Bi^{5+} ions in these compounds. A non-adiabatic hopping model of small polarons has been used to explain this behaviour and the variable valence character of Bi substitute has been experimentally established using XPS spectra of these hexaferrites to calculate the Bi^{5+} to Bi^{3+} ions ratio[10]. The XPS spectra of $BaO5.6\ Fe_2O_30.4\ Bi_2O_3$ samples showed distinct split in the $4f_{7/2}$ and $4f_{5/2}$ lines (Figure 5) showing the mixed valence states and the ratio was determined by calculating the ratio of area under the split curves. Similar XPS spectra were obtained for $Ni_{0.5}\ Zn_{0.5}\ Bi_{0.15}\ F_{1.85}\ O_4$ nickel–zinc ferrite composition showing similar split in Bi $4f_{7/2}$ and $4f_{5/2}$ lines[11]. These investigations show that the presence of variable valence bismuth ions brings about an increase in Fe^{2+} concentration which is believed to cause an increase in electrical conductivity in these samples.

Secondary ion mass spectrometry

SIMS investigations on surface contamination of Pt–Ir alloy used for standard kilogram: The national prototype standard kilogram mass made of Pt(90%)–Ir(10%) alloy artifact shows a mass increase trend during intercomparison with the international prototype kept at

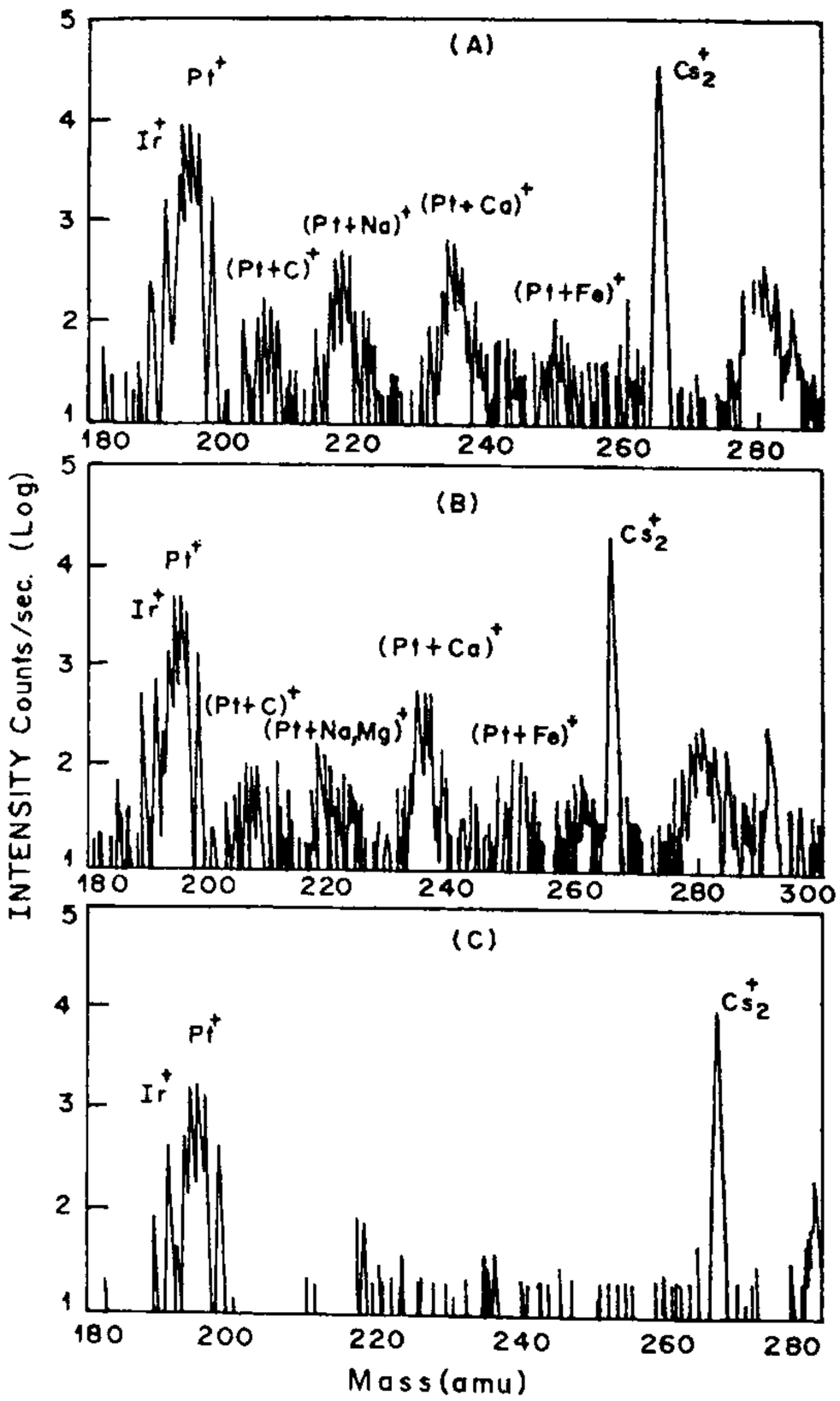

Figure 6. SIMS spectra (180–280 amu) obtained *a*, before cleaning; *b*, after cleaning; and *c*, after sputtering the cleaned Pt–Ir alloy sample.

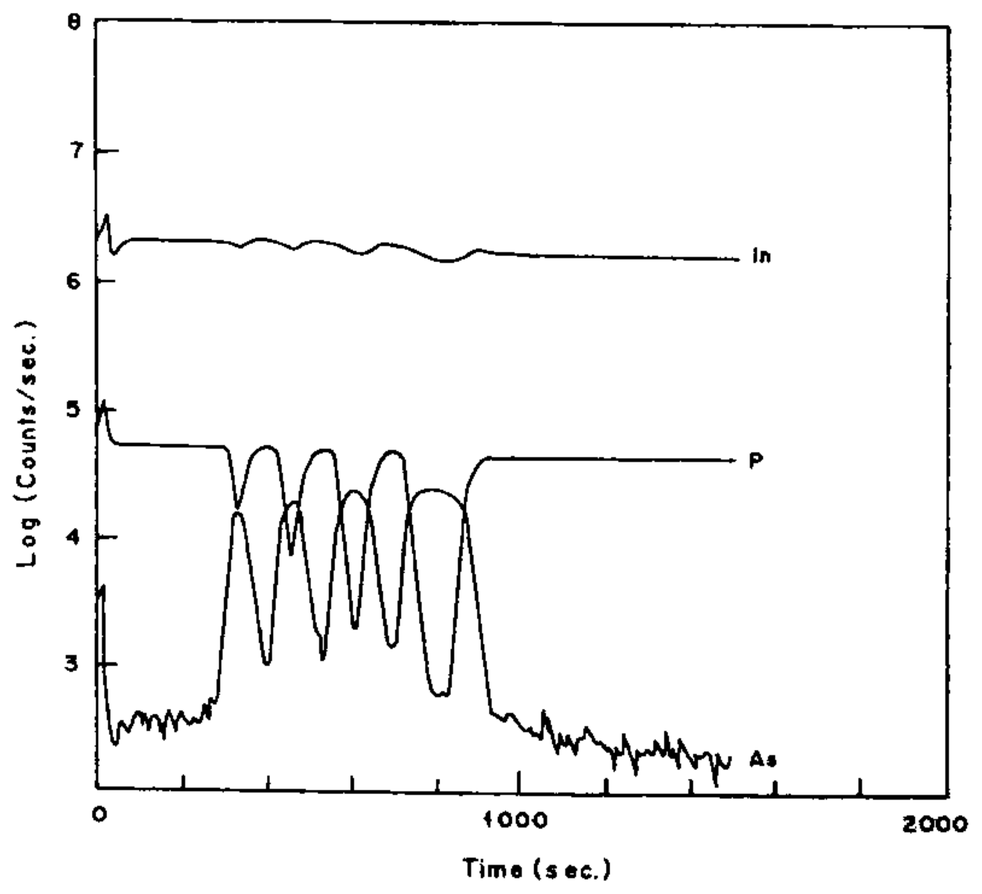

Figure 7. Depth profile of InP/InGaAs ... multilayer structure using O_2^+ at 7.0 KeV primary beam. The P profile shows the different well widths in increasing order. The abscissa is sputtering time and one can convert this into depth by measuring crater depth with a profilometer.

BIPM, France, after the prescribed cleaning procedure. Using SIMS for surface analysis it was observed[12] that most of the contaminants like oxygen, Mg, Ca, C, Na and hydrocarbons increase immediately after solvent cleaning while they reduce considerably if only steam jet cleaning is adopted (Figure 6). Impurities like Na, Mg and Ca were found even inside the bulk up to a depth of 300 nm which may have diffused through the defects such as grain boundaries and dislocations produced due to diamond machining of the sample surface. It was concluded that only steam cleaning might be recommended for the stability of the mass material compared to other cleaning methods where solvents are used. Further work using a static SIMS[13] confirmed that various oxygenated and non-oxygenated hydrocarbons get absorbed immediately after solvent cleaning providing a scenario for the increase in mass after standard cleaning procedure.

Measurement of well widths of MOVPE grown InGaAs/InP quantum wells using SIMS: InGaAs/InP quantum wells with varied thicknesses were grown by MOVPE technique at IIT, Kharagpur and the well widths were measured by NPL SIMS using depth profiling. The depth profile for quantum well structures was carried out with an O_2^+ primary beam. The sputtering parameters, viz. the beam energy, the incident angle, beam current, etc. were optimized to get a low sputtering rate of 0.1 nm/sec and the depth resolution was found to be between 2 and 3 nm. The preferential sputtering rates of InP and InGaAs were also later normalized for the well depth calculations using standard samples of InP and InGaAsP.

Figure 7 gives the depth profile of the quantum well structure at 625°C which showed the best sharpness in the interface compared to those grown at 610°C and 640°C. The detailed SIMS work is being published elsewhere[14] showing a number of such samples grown at different temperatures and with equal or varied widths ranging from 2 nm to 30 nm along with some Photoluminescence (PL) and cross-section Transmission Electron Microscopy (XTEM) results.

Conclusions

A series of fundamental research work has been undertaken using LEED, EELS, AES, XPS and SIMS, established at the Surface Physics group in NPL, to understand the fundamental processes at the surfaces and interfaces of metals and semiconductors. The growth kinetics, chemical state determination with charge transfer mechanism, catalytic role of different metal or semiconductor materials and multilayer structures have been studied using the above techniques. The facility available at the group also serves as a centre for different relevant industries or R&D institutions of the country.

1. Sharma, J. K. N., Mohan, P. and Sharma, D. R., *J. Vaccum Sci. Technol. A*, 1990, **8**, 941–947.
2. Mohan, P., *Vacuum*, 1998, **51**, 69–74.
3. Mohan, P. and Gupta, A. C., *Vacuum*, 1997, **48**, 515–519.
4. Sharma, J. K. N., Chakraborty, B. R. and Shivaprasad, S. M., *Surf. Sci.*, 1993, **285**, 237.
5. Bera, S., Shivaprasad, S. M. and Sharma, J. K. N., *Appl. Surf. Sci.*, 1994, **74**, 13.
6. Shivaprasad, S. M., Singh, S. and Aparna, Y., *Solid State Commun.*, 1998, **107**, 257.
7. Shivaprasad, S. M., Bera, S. and Aparna, Y., *Bull. Mater. Sci.*, 1998, **21**, 111.
8. Shivaprasad, S. M., Anandan, C., Azatyan, S. G., Gavriljuk, Y. L. and Lifshits, V. G., *Surf. Sci.*, 1997, **382**, 258.
9. Singh, S., Shivaprasad, S. M. and Anandan, C., *Appl. Surf. Sci.*, 1998, **136**, 189.
10. Pal, M., Brahma, P., Chakraborty, B. R. and Chakraborty, D., *Jpn J. Appl. Phys.*, 1997, **36**, 2163.
11. Pal, M., Brahma, P., Chakraborty, D., Chakraborty, B. R., Anandan, C. and Bera, S., *J. Mater Sci. Lett.*, 1998, **16**, 270.
12. Sharma, D. R., Chakraborty, B. R. and Das, M. L., *Appl. Surf. Sci.*, 1998, **135**, 193.
13. Chakraborty, B. R., Lehman, D. E. and Winograd, N., *Rapid Commun. Mass Spectrom.*, 1998, **12**, 1261.
14. Bose, D. N., Banerjee, P., Bhunia, S. B., Aparna, Y., Chhetri, M. B. and Chakraborty, B. R., *Appl. Surf. Sci.*, in press.

ACKNOWLEDGEMENT. The Surface Physics group thanks the US-Government (INDO-US Project), United Nations Development Programme (UNDP) and CSIR for the financial support provided to establish the Surface Analytical Facility (SAF) at NPL, New Delhi.